
Journal of Informatics and Web Engineering

Vol. 4 No. 1 (February 2025)

eISSN: 2821-370X

Lung Tumor Segmentation in Medical Imaging Using U-NET

J Jayapradha^{1*}, Su-Cheng Haw², Naveen Palanichamy³, Senthil Kumar Thillaigovindhan⁴,
Mutaz Al-Tarawneh⁵

^{1,4}Department of Computing Technologies, School of Computing, SRM Institute of Science and Technology,
Kattankulathur, Tamil Nadu 6030203, India

^{2,3}Faculty of Computing and Informatics, Multimedia University, Persiaran Multimedia, 63100 Cyberjaya,
Malaysia.

⁵Faculty of Engineering, Mutah University, Street Mu'tah, Karak 61710 Jordan

*corresponding author: (jayapraj@srmist.edu.in; ORCID: 0000-0002-2548-9135)

Abstract— Tumors are a deadly condition often triggered by a range of abnormal modifications and genetic abnormalities. Early tumor diagnosis is essential due to the highly concerned nature of the disease. Early detection and treatment of tumors can significantly reduce mortality rates. This paper presents a model for tumor segmentation in medical imaging that uses the U-NET architecture to increase precision. The model's encoding and decoding processes have been applied with skip connections to boost performance while simplifying model training. Images were cropped around the lower abdominal regions, and all images used in the study were then resized to 256*256 pixels for standardization. The proposed model deals with the class imbalance using data augmentation and oversampling. The experiments achieved a dice score of 0.853 ± 0.02 ; F-score of 0.905 ± 0.02 ; and a sensitivity of 0.897 ± 0.02 , compared with various existing models. As part of the model's application, the pytorch-lightning library is used to successfully identify lung cancer scans, thereby proving to be a precise and efficient method of tumor identification. Accordingly, the study emphasizes the accuracy and speed of the applied model as a useful instrument for the earliest detection of tumors. The proposed approach helps to achieve more relevant and accurate segmentation and thus provides enhancements in medical images analysis if such challenges as an imbalance data set are well handled.

Keywords—Lung Tumor, U-Net, Pytorch-lightning, Segmentation, Data Augmentation.

Received: 19 October 2024; Accepted: 19 December 2024; Published: 16 February 2025

This is an open access article under the [CC BY-NC-ND 4.0](https://creativecommons.org/licenses/by-nc-nd/4.0/) license.



1. INTRODUCTION

The term "cancer" refers to the formation of cells that are not under control and compatible with normal cell function [1]. Cancer, the second largest cause of death worldwide, is currently one of the most significant challenges that the public health sector is presently confronting. A total of 238,340 people, including 117,550 men and 120,790 women, are anticipated to be diagnosed with lung cancer in the year 2023. In addition, it is estimated that 127,070 people died because of the ailment. If lung cancer is discovered early, there is a significantly enhanced chance of successful therapy. Lung cancer has a devastating effect on millions of people and requires lifetime medical attention [2]. It is of utmost importance to facilitate the anticipated prognosis and exactitude of lung cancer therapy through early detection



Journal of Informatics and Web Engineering

<https://doi.org/10.33093/jiwe.2025.4.1.11>

© Universiti Telekom Sdn Bhd.

Published by MMU Press. URL: <https://journals.mmupress.com/jiwe>

and diagnosis. Lung cancer leads to the highest mortality rates worldwide [3], [4]. Although lung cancer is considered the most severe type of a cancer, it is important to note that early detection of such cancer has a higher possibility of successful treatment. Additionally, this type of development can trigger metastasis, a phenomenon that involves the attachment of the cancerous cells to other tissues and the spread of the cancerous cells beyond the region of the lungs [5]. A significant number of criteria, including patient effectiveness, histological cancer type, and the degree of cancer malignancy, are the primary elements that determine the therapy and diagnosis. In computed tomography (CT), CT images generate perfect detailing of the human body parts, and these images have been employed as a non-invasive model for detecting and observing many types of illness. Moreover, CT imaging has modernized traditional medical imaging methods, providing accurate elements for generating the internal bodies and aiding in vital clinical decisions [6],[7]. The primary objective of the proposed work is to present a model for tumor segmentation in CT medical images using U-Net architecture. The paper is organized as follows: Section 2 discusses the related work, and Section 3 addresses the implementation of the proposed model. The experimental results are discussed and compared with the existing models in Section 4 and finally the Section 5 concludes the paper with future enhancement.

2. LITERATURE REVIEW

Nearly 80% of individuals diagnosed with lung tumors are not eligible for surgical intervention [8]. The primary course of treatment for these patients involves a combination of chemotherapy and radiotherapy; precise tumor localization is essential for radiotherapy and the assessing its effectiveness [9]. CT is the primary imaging technique utilized for finding, ray planning, and prediction. Typically, specialists manually outline the treatment target on CT scan and then upload it to a treatment planning system for radiation dosage calculation [10]. In addition, the effectiveness of treatment can typically be assessed by evaluating alterations in tumor size, commonly with one-dimensional assessment techniques, such as RECIST v1.1. Tumor segmentation is also necessary for contemporary popular radiomics research hence, tumor segmentation has a broad spectrum of uses in lung cancer. The process of manually outlining the tumor is arduous, time-onerous, biased, and exhibits significant diversity among different observers as well as within the same observer. Hence, the implementation of automatic segmentation techniques is crucial to alleviate the capacity of radiologists and enhance the objectivity of the segmentation outcomes.

In recent years, there has been a significant progression in automatic medical image segmentation with the advance of fully convolutional neural network architectures (FCNNs) [11]. The U-Net [12] is an example of an encoder-decoder design that includes an encoder, decoder, and lengthy skip links at every resolution level. The primary objective is to merge the encoder's high-resolution characteristics with the matching decoder's up-sampling characteristics to integrate multiscale data. Isensee et al. [13] recently introduced nn-Unet as a modification of U-Net. Based on deep learning, this segmentation approach can autonomously adjust parameters, such as preprocessing, network topology, and training strategy and also demonstrated exceptional performance in several tasks, surpassing current benchmarks. The study relied on spectral data collection via deep learning, which correctly predicted lung tumors from the input data and illustrated the ability to combine deep learning and pipelining techniques as an efficient approach to boost the computer system's performance for detecting lung tumors [14].

In [15],[16],[17], the mechanism describes the development of bone metastasis, such that the lungs can possibly obtain tumors. Toxicities observed in the late stages of the tumor are a manifestation of delayed Toxicity sequelae. The osteolytic disease affects around 10-15% of individuals in the cases of lung tumors. CSF non-tumor cells that enter the thoracic spine from the neck/back, may reach the spinal cord and cause both back pain with neurological complications [18]. CT imaging with energy/spectral parameters is a multimodal image generation method made by spiral and multislice CT. CT has such excellent imaging capability that it can simultaneously detect and display several parameters [19],[20].

Deep learning is the implementation of Artificial Neural Networks (ANN) that imitate human thinking to process information [21],[22]. Artificial Neural Networks (ANN) is a class of nonlinear processing that includes brain capacity distribution to devices' memory, parameters, and turning completeness. The Machine Learning algorithms demonstrate the procedures and costs that are set continuously [23]. Pulverization is performed through a two-layer approach primarily based on receptive field constriction and feature map expansion.

3. IMPLEMENTATION OF THE PROPOSED MODEL

U-Net is a primary segmentation model, and the U-Net architecture is built on the idea of feature pyramid and skip connections. In the encoder phase, downsampling the convolutional layers reduce the field of view and gradually extract progressive abstraction of the input data. The encoded attributes play a significant role in the contextual information to support segmentation. On the other hand, the decoder phase is focused solely on reconstructing the initial input shape: taking features that appear during the encoder phase. Finally, the decoder part applies sampling operations to raise the dimensions of the feature maps and make them like the input dimensions. This process is performed iteratively to optimize the segmentation mask by minimizing the energy cost threshold. When using skip connections, it becomes possible to directly pass on information from the encoder to the decoder without erosion of hard-to-capture spatial details over different resolutions. For a better flow of information path between encoder and decoder, they use skip connections such that the segmentation masks generated using U-Net possess good quality. The enhancements introduced through the U-Net design benefit the training process by alleviating doubts about information loss and gradient vanishing, thereby leading to better general convergence and higher segmentation performance. The proposed model comprises the following steps 1) Pre-processing (Normalization & Slicing), 2) Data Augmentation, 3) Implementation of U-Net and 4) segmentation, as shown in Figure 1.

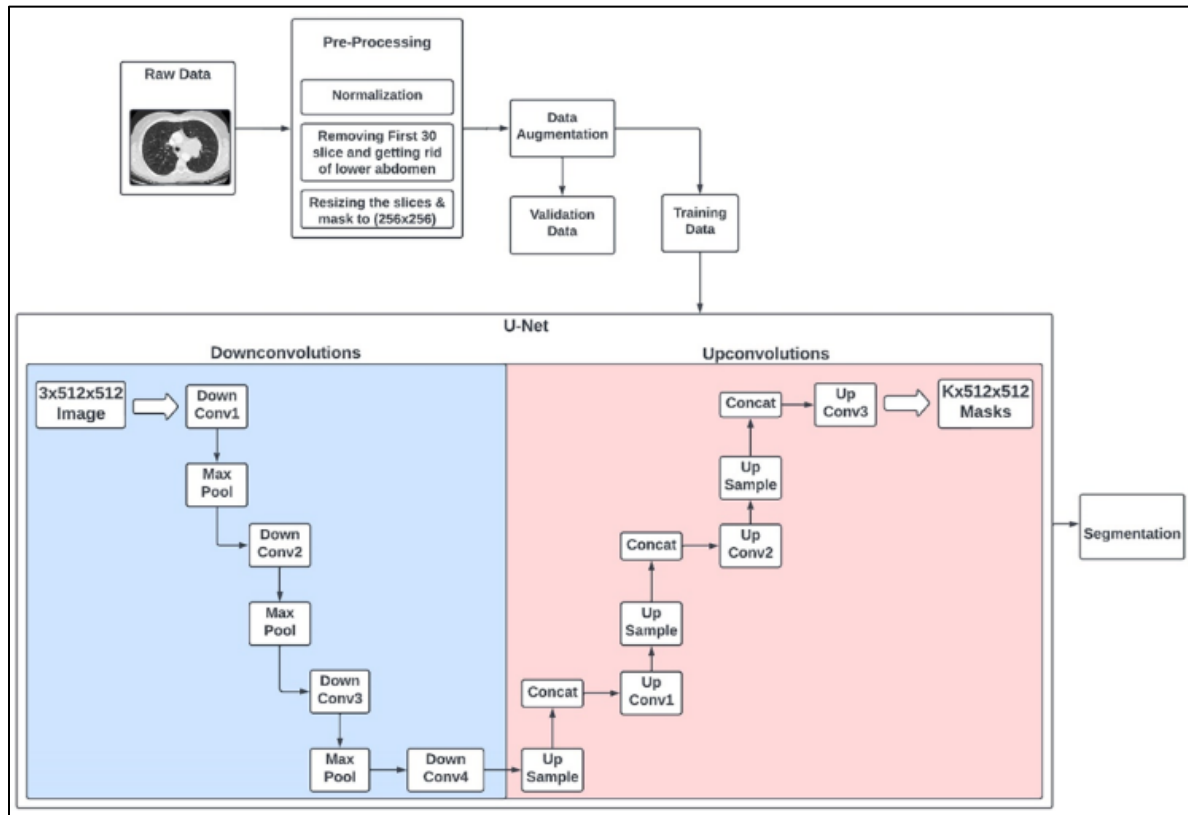


Figure 1. Architecture Diagram of The Model

3.1 Preprocessing

In the proposed model, the Task06_lung.tar dataset from Medical Segmentation Decathlon (<http://medicaldecathlon.com/>) was used. The dataset contains 15,767 samples. A total of 12613 samples were used for training, and 3154 were used for testing. The computational efficiency of preprocessing CT images for the identification of lung tumors is improved in the proposed model. The following strategies focus on crucial anatomical locations in pre-processing techniques.

Normalization: A data pre-processing technique used to convert the aspects of the images to a normal range to enhance the execution and accuracy of ML algorithms. The primary purpose of normalization is to eliminate the range of probable predispositions and distortions. The images were normalized by dividing them by 3071, which is the typical range of values from -1000 to 3071 Hounsfield Unit (HU). This obviates the need to calculate the average and standard deviation of images. The implemented normalization is given below as Equation (1).

$$CT_{data} = CT_{data}[:, :, 30:] / 3071 \quad (1)$$

Slicing: The proposed model works only on 2D datasets. The first 30 slices are 3D, they are removed from the dataset and saved in two-dimensional files to accelerate processing. It is performed as loading individual slices is significantly quicker than processing entire NIfTI files. The purpose of slicing is to concentrate on analyzing individual slices rather than analyzing subjects, comparing 2D analysis to 3D analysis. The slicing of the images is shown in Equation (2).

$$newlabel_{data} = newlabel_{data}[:, :, 30:] \quad (2)$$

Furthermore, to streamline the learning process and prioritize the assessment of lung tumors, sections of the lower abdomen are excised, thereby reducing complexity. Concentrated learning may be promoted by omitting the first thirty portions, which extend from the lower belly to the neck. The size of the slices and masks was set to be (256, 256), which makes it easier for future research and comparisons. The mask resizing process uses the nearest neighbor interpolation approach to maintain the integrity of the data and ensure accurate mask resizing as shown in Equations 3 and 4. These preprocessing algorithms optimize the computing resources and prioritize crucial anatomical data to diagnose lung tumors, individually and collectively effectively.

$$slice = cv2.resize(slice, (256, 256)) \quad (3)$$

$$image_{mask} = cv2.resize(image_{mask}, (256, 256), int_{pol} = cv2.int_{near}) \quad (4)$$

3.2 Data Augmentation

Data augmentation is an important concept in the field of learning that involves creating synthetic data from a given set of data samples. This process is particularly useful when handling the problem of working with an imbalanced dataset and enhancing the ability to generalize for various uses. The easy capture phase involves scanning the entire domain for all 2D parts and conglomerating a large database to build a comprehensive inventory of all two-primary dimensional components across many domains. Then, each slice route is aligned with its corresponding label path to ensure that the picture data and annotations are aligned with each other. Next, these slices and labels are incorporated into the present system to feed the system with the necessary data for subsequent analysis. The dataset is made more diverse, and its variability is enhanced using various procedures, which involve a range of changes including rotation, flipping, scaling, and affine transformations, among others. Data augmentation enhances the model's ability to detect lung cancers in different environments in terms of appearance and image structure, as shown in Equation (5).

$$random_{seed} = torch_{randint}(0, 1000000, (1,))[0].item()imgaug_{seed}(random_{seed}) \quad (5)$$

After the end of the data augmentation process, the changed slices and masks are given to increase their possibilities of being incorporated into the training process. Data augmentation ensures that the extended data is readily accessible for both model training and evaluation. This will facilitate the iterative improvement and optimization of the algorithm used for detecting lung tumors. Systematic implementation of these functionalities is crucial for successfully developing and deploying reliable lung cancer detection systems.

The segmentation model applied to the entire lung tumor detection model is significant when working with PyTorch Lightning. Thus, the proposed framework provides an optimized environment to build, educate, and invent models to ensure success and expansiveness. When implementing the above, a suitable approach must be used to counter the class imbalance that is more often exhibited in detecting lung tumors.

To overcome this challenge, oversampling approaches are employed that follow equal importance to all slices, wherein slices having tumors are given importance to ensure adequate representation from each class. The WeightedRandomSampler from PyTorch makes this process easier by assigning the most appropriate weights to the samples in the dataset to enhance learning even beyond cases of class imbalance.

4. RESULTS AND DISCUSSIONS

The proposed model, which uses the U-Net architecture and PyTorch Lightning developed for the identification of lung tumors, exhibits the highest accuracy and reliability. The neural network processes the cancerous CT images and recognizes the correct cancer tumor using intense preprocessing procedures like normalization, cropping, and scaling. The model employs over-sampling methods to address class imbalances and then optimizes the utilization of the Binary Cross Entropy function as the loss function. The confusion matrix shown in Figure 2 results in pixel format. The true positive to false negative ratio was approximately 91.6%, which is a very high accuracy result. Similarly, in the case of true-negative to false positive, the ratio is close to 99.9% which shows that it will most likely never show the false-negative tumor. Equations (6) to (11) show the calculated values in the confusion matrix.

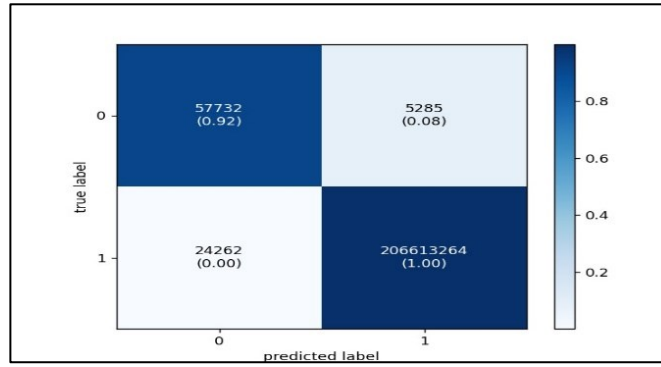


Figure 2. Confusion Matrix

$$T_p = \text{int}((P_b * M_b).sum().item()) \quad (6)$$

$$F_p = \text{int}(((P_b - M_b) > 0).sum().item()) \quad (7)$$

$$F_N = \text{int}((M_b - P_b > 0).sum().item()) \quad (8)$$

$$T_N = \text{int}(((1 - P_b) * (1 - M_b)).sum().item()) \quad (9)$$

where,

$$P_b = (\text{pred} > 0.5).float() \quad (10)$$

$$M_b = (\text{mask} > 0.5).float() \quad (11)$$

Here, T_p is the True positive, F_p is the False positive, F_N is the False Negative, T_N is the True Negative, P_b is `pred_binary`, and M_b is `Mask_binary`. Figure 3(a) on the left shows the initial CT scan with a pixel intensity of 512×512 and Figure 3(b) on the right shows the preprocessed image after it has been cropped and normalized to 256×256 pixels. This preprocessing simplifies the dataset to only core areas so that the U-NET model solves the tumor detection problem more effectively and efficiently.

The Dice score findings prove that the proposed model is very competitive. The module aptitude of our solution was 0.853 ± 0.02 , which indicates a high degree of reliability in terms of correctly segmenting lung tumors in CT scans. The formula used for the dice score is shown in Equation (12).

$$\text{dice} = (2 * \text{counter}) / \text{denum} \quad (12)$$



(a) (b)

Figure 3. (a) Original CT, (b) Preprocessed

Because it is a segmentation model, the algorithm demonstrated a high level of accuracy, achieving a rate of $99.8\% \pm 0.02\%$ as it is calculated based on the number of frames the tumor is detected not the complete CT scan image, as shown in Figure 4. The system's high accuracy rate demonstrates its effectiveness in detecting minor abnormalities in medical images, which improves diagnostic accuracy. The proposed model's unique feature is that it has a specificity of $.99 \pm 0.02$ and a sensitivity of 0.897 ± 0.02 as shown in Figure 5. This demonstrates that the proposed model can capture true positives and real negatives and minimize expected false negatives. This revealed the reliability by distinguishing points of interest and delimiting the objects of interest in the specified dataset. The U-net based cell carcinoma segmentation' model, however, demonstrates a slightly lower specificity of 0.970 but together with a higher sensitivity of 0.972 seems to possess a remarkable capacity to detect true positives that are less likely to be misclassified than negatives. At the same time, there is a higher chance of occasional false positives. This shows that the model has a good degree of precision and efficiency in picking those instances of interest that are of importance and at the same time, balancing the cases mainly composed of negative and positive ones.

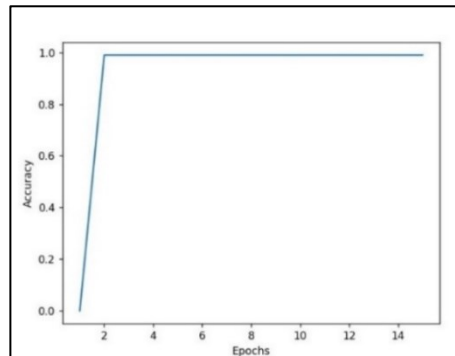


Figure 4. Epoch-wise Accuracy Variation

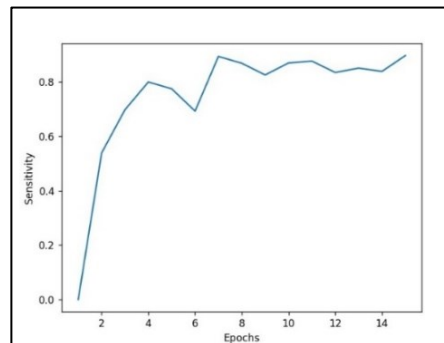


Figure 5. Epoch-wise Sensitivity Variation

It becomes a reliable tool for correct categorizing positive and negative cases. The proposed model stands out in this field for its high accuracy rate and beyond recall. Therefore, this sample can be applied to workplaces that require the balanced identification of false positives and genuine positives. After measuring the F-score and accuracy of our proposed model which displays 0.905 ± 0.02 F-score and 0.91 ± 0.02 precision as shown in Figures 6 and 7.

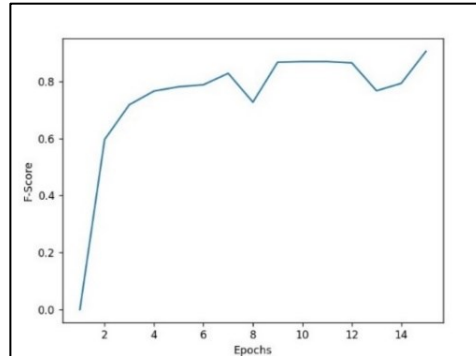


Figure 6. Epoch-wise F-Score Variation

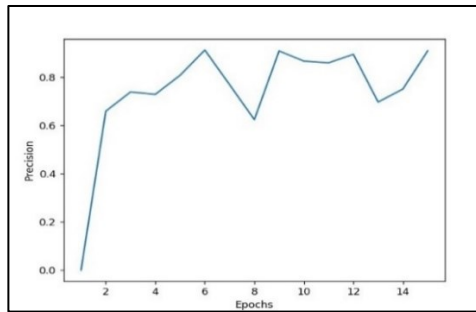


Figure 7. Epoch-wise Precision Variation

These statistics confirm the effectiveness of the model for data categorization together with low false positive and negative results. From Figure 6, there is an evident increase in the F-score level as the training epochs increases which shows that the model composed an effective learning paradigm based on the given training data. This gradual increase in performance proves the fact that the training process of the model is very stable and reliable. Altogether, these results support the proposed model and state that it provides high accuracy and recall values to yield precise and accurate results of the medical imaging segmentation tasks. The precision of the proposed model is calculated at ± 0.91 and the ± 0.02 signifies that the proposed model can select true positive efficiency with minimum false positive cases. Figure 7 is also a good representation having an indication that there is a positive correlation between the number of training epochs and the precision. This enhancement is influenced by the understanding that the model adapts over time in the sense that it gains the capacity to capture details or new characteristics into the data required to make better decisions. The gradually increasing level of precision demonstrates the effectiveness of training and proves the efficiency of created models in solving complex tasks like tumor recognition in the radiological images.

4.1 Comparing U-NET with Other Models

The criteria for measuring the efficiency of the tumor segmentation models were the Dice score, F-Score, Sensitivity and Convergence. The Dice Score compares the predicted tumor regions against the actual or ground truth regions and provides insight into segmentation quality. The F-Score combines Matthew Butterfly's precision with the E-Score's recall, demonstrating how accurate the model is in recognizing false positives and false negatives. Sensitivity measures the accuracy of the model in correctly identifying true positives, a sign of good tumor segmentation. Finally, we used the loss function to compute convergence across the training epochs, which shows when the model starts to converge and provides optimal performance. These metrics in combination offer the best way to assess model performance in tumor diagnosis. Table 1 compares the performance parameter values.

Table 1. Comparison of the Performance Parameters

Model	Dice Score	F-Score	Sensitivity	Convergence (Loss after 10 epochs)
U-NET	0.853 \pm 0.02	0.905 \pm 0.02	0.897 \pm 0.02	0.25 (BCE)
FCN	0.82 \pm 0.03	0.88 \pm 0.03	0.85 \pm 0.03	0.35
SegNet	0.80 \pm 0.03	0.86 \pm 0.02	0.83 \pm 0.03	0.38
DeepLabV3	0.84 \pm 0.02	0.89 \pm 0.02	0.88 \pm 0.02	0.27

4.1.1 Discussion

Dice Score Comparison

The U-NET model was given a Dice Score of 0.853, thereby showing that the proposed model is equally as efficient as DeepLabV3 as given the Dice Score of 0.84 for predicting the tumor regions with high conformity. FCN is slightly behind a Dice Score of 0.82 and SegNet having a Dice Score of 0.80, which suggests that U-NET and DeepLabV3 can maintain a stronger spatial relation. This is because skip connections and deeper architectures were utilized to improve their performance on the segmentation of features such as tumors.

F-Score Comparison

Comparing the F-Score of the U-NET model with that of DeepLabV3, it was 0.905 for U-NET, we can see that U-NET gives nearly the high accuracy as DeepLabV3 and has a brilliant ability to influence precision and recall giving an optimal decision for segmentation of tumor regions without leading to over or under-estimation. FCN has an F-Score of 0.88 and SegNet has an F-Score of 0.86 lower than U-Net implying that these models might have high false positives or false negatives and hence lower tumor detection reliability.

Sensitivity Comparison

DeepLabV3 has a sensitivity of 0.88, whereas U-NET has a sensitivity of 0.897; this suggests that U-NET does better than DeepLab for distinguishing true positives and outlining real tumor areas. On the other hand, FCN (sensitivity 0.85) sensitivity is less than the proposed network, and SegNet (sensitivity 0.83) is also less sensitive meaning that FCN and SegNet are more likely to overlook true tumor regions and therefore not as effective in detecting all the areas of the tumor.

Convergence (Loss) Comparison

U-NET model with a final loss of 0.25 using BCE Loss converges faster than SegNet which has a loss of 0.38, FCN with a loss of 0.35. By using BCE Loss instead of Dice Loss, the optimization of the pixel-wise prediction is faster, which optimizes the U-NET model's convergence.

Considering this result, U-NET is efficient in tumor segmentation tasks as shown in Figure 8. U-NET had a slightly higher average Dice Score and Sensitivity score than the DeepLabV3. DeepLabV3 has less computational time and complexity because of the small layer size. The implementation of skip connections also guarantees the retention of spatial features while at the same time keeping the model more restrained; hence, thus, it be used to serve various applications even where computational power is limited.

However, comparatively easy models, such as FCN and SegNet are less effective, but still not able to compete with U-NET and DeepLabV3, especially in the case of the segmentation of more intricate tumors and the problem of class imbalance. Their structures are relatively plain; thus, there are no skip connections or convolutions, which are crucial for properly segmenting the tumor area if the set contains many samples with a significant difference between the tumor area and the rest of the organ. This means that the Dice scores of FCN and SegNet achieve are reduced, as are Sensitivity and the F-score. Therefore, U-NET offers a reasonable compromise between accuracy and training time and could be used in many medical imaging tasks. Although it is relatively heavier, it ultimately provides the highest overall performance; hence, has been preferred for all those tasks where precision is a key to success as well as where

enormous power of computation is not a constraint. These comparisons illustrate the potential compromises that must be made when choosing a segmentation model depending on the value being emphasized, speed, or accuracy.

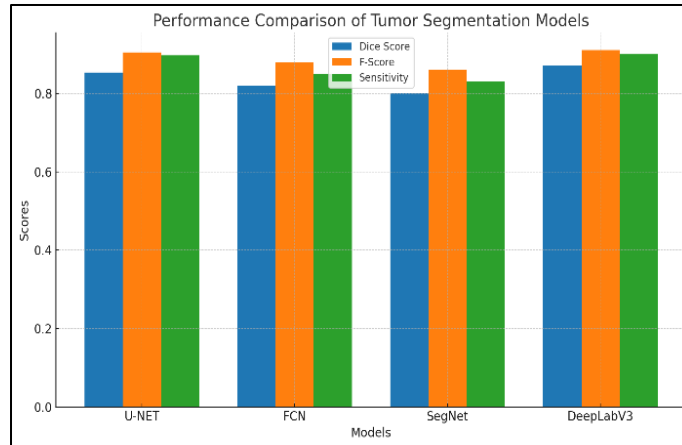


Figure 8. Performance Comparison of Tumor Segmentation Model

5. CONCLUSION AND FUTURE ENHANCEMENT

Another breakthrough in the medical imaging field is the application of U-Net architectures for detecting lung tumors. By implementing normalization, cropping, and resizing with PyTorch Lightning can achieve accurate segmentation of tumors from CT-scanned modalities. A high Dice similarity score of 0.853 ± 0.02 is shown proving that the proposed model can be useful for the early detection and treatment planning of cancer. Exploring enhanced data augmentation techniques can enhance the model learning capabilities of different imaging environments. Superimposing two or more imaging data modalities, such as CT with MR could be beneficial in tumor detection algorithms improvement due to variations in the type and sensitivity of the imaging data. Moreover, presenting a simple alteration or extension of the U-net architecture or adding new state-of-the-art deep learning methods can offer a new horizon toward improving the efficiency and precision of the segmentation model. Finally, validation studies must involve as many patients and clinical settings as possible to understand the operational usability of the created algorithms. This should help in their adoption and implementation across all healthcare practicum.

ACKNOWLEDGEMENT

The authors wish to thank all party that have directly or indirectly contributed to this article.

FUNDING STATEMENTS

The authors received no funding from any party for the research and publication of this article.

AUTHOR CONTRIBUTIONS

J Jayapradha: Conceptualization, Data Curation, Methodology, Validation, Writing – Original Draft Preparation.

Su-Cheng Haw: Project Administration, Writing – Review & Editing.

Naveen Palanichamy: Project Administration, Supervision, Writing – Review & Editing.

Senthil Kumar Thillaigovindhan: Conceptualization.

CONFLICT OF INTERESTS

No conflict of interests was disclosed.

ETHICS STATEMENTS


Our publication ethics follow The Committee of Publication Ethics (COPE) guideline. <https://publicationethics.org/>



REFERENCES

- [1] H. F. Al-Yasriy, M. S. AL-Husieny, F. Y. Mohsen, E. A. Khalil, and Z. S. Hassan, "Diagnosis of Lung Cancer Based on CT Scans Using CNN," *IOP Conference Series: Materials Science and Engineering*, vol. 928, no. 2, p. 022035, Nov. 2020, doi: 10.1088/1757-899X/928/2/022035.
- [2] M. G. Mokwena, C. A. Kruger, M.-T. Ivan, and A. Heidi, "A review of nanoparticle photosensitizer drug delivery uptake systems for photodynamic treatment of lung cancer," *Photodiagnosis and Photodynamic Therapy*, vol. 22, pp. 147–154, Jun. 2018, doi: 10.1016/j.pdpdt.2018.03.006.
- [3] K. S. Pradhan, P. Chawla, and R. Tiwari, "HRDEL: High ranking deep ensemble learning-based lung cancer diagnosis model," *Expert Systems with Applications*, vol. 213, p. 118956, Mar. 2023, doi: 10.1016/j.eswa.2022.118956.
- [4] J. Zhang *et al.*, "Establishment of the prognostic index of lung squamous cell carcinoma based on immunogenomic landscape analysis," *Cancer Cell International*, vol. 20, no. 1, p. 330, Dec. 2020, doi: 10.1186/s12935-020-01429-y.
- [5] P. P. R. Filho *et al.*, "Automated recognition of lung diseases in CT images based on the optimum-path forest classifier," *Neural Computing and Applications*, vol. 31, no. S2, pp. 901–914, Feb. 2019, doi: 10.1007/s00521-017-3048-y.
- [6] M. Ragab, I. Katib, S. A. Sharaf, F. Y. Assiri, D. Hamed, and A. A.-M. Al-Ghamdi, "Self-Upgraded Cat Mouse Optimizer With Machine Learning Driven Lung Cancer Classification on Computed Tomography Imaging," *IEEE Access*, vol. 11, pp. 107972–107981, 2023, doi: 10.1109/ACCESS.2023.3313508.
- [7] H. Sung *et al.*, "Global Cancer Statistics 2020: GLOBOCAN Estimates of Incidence and Mortality Worldwide for 36 Cancers in 185 Countries," *CA: A Cancer Journal for Clinicians*, vol. 71, no. 3, pp. 209–249, May 2021, doi: 10.3322/caac.21660.
- [8] S. Maurya, S. Tiwari, M. C. Mothukuri, C. M. Tangeda, R. N. S. Nandigam, and D. C. Addagiri, "A review on recent developments in cancer detection using Machine Learning and Deep Learning models," *Biomedical Signal Processing and Control*, vol. 80, p. 104398, Feb. 2023, doi: 10.1016/j.bspc.2022.104398.
- [9] J.-J. Sonke and J. Belderbos, "Adaptive Radiotherapy for Lung Cancer," *Seminars in Radiation Oncology*, vol. 20, no. 2, pp. 94–106, Apr. 2010, doi: 10.1016/j.semradonc.2009.11.003.
- [10] G. Sharp *et al.*, "Vision 20/20: Perspectives on automated image segmentation for radiotherapy," *Medical Physics*, vol. 41, no. 5, p. 050902, Apr. 2014, doi: 10.1118/1.4871620.
- [11] C. C. Chai, W. H. Khoh, Y. H. Pang, and H. Y. Yap, "A Lung Cancer Detection with Pre-Trained CNN Models," *Journal of Informatics and Web Engineering*, vol. 3, no. 1, pp. 41–54, Feb. 2024, doi: 10.33093/jiwe.2024.3.1.3.
- [11] Ronneberger, P. Fischer, and T. Brox, "U-Net: Convolutional Networks for Biomedical Image Segmentation," 2015, pp. 234–241. doi: 10.1007/978-3-319-24574-4_28.
- [12] F. Isensee, P. F. Jaeger, S. A. A. Kohl, J. Petersen, and K. H. Maier-Hein, "nnU-Net: a self-configuring method for deep learning-based biomedical image segmentation," *Nature Methods*, vol. 18, no. 2, pp. 203–211, Feb. 2021, doi: 10.1038/s41592-020-01008-z.
- [13] P. M. Shakeel, M. A. Burhanuddin, and M. I. Desa, "Lung cancer detection from CT image using improved profuse clustering and deep learning instantaneously trained neural networks," *Measurement*, vol. 145, pp. 702–712, Oct. 2019, doi: 10.1016/j.measurement.2019.05.027.
- [14] H. H. Popper, "Progression and metastasis of lung cancer," *Cancer and Metastasis Reviews*, vol. 35, no. 1, pp. 75–91, Mar. 2016, doi: 10.1007/s10555-016-9618-0.

- [15] K. Cetin, C. F. Christiansen, J. B. Jacobsen, M. Nørgaard, and H. T. Sørensen, "Bone metastasis, skeletal-related events, and mortality in lung cancer patients: A Danish population-based cohort study," *Lung Cancer*, vol. 86, no. 2, pp. 247–254, Nov. 2014, doi: 10.1016/j.lungcan.2014.08.022.
- [16] K. L. Lew, C. Y. Kew, K. S. Sim, and S. C. Tan, "Adaptive Gaussian Wiener Filter for CT-Scan Images with Gaussian Noise Variance," *Journal of Informatics and Web Engineering*, vol. 3, no. 1, pp. 169–181, Feb. 2024, doi: 10.33093/jiwe.2024.3.1.11.
- [17] Q. Xu, M. Li, M. Li, and S. Liu, "Energy Spectrum CT Image Detection Based Dimensionality Reduction with Phase Congruency," *Journal of Medical Systems*, vol. 42, no. 3, p. 49, Mar. 2018, doi: 10.1007/s10916-018-0904-y.
- [18] G. Wang, D. Zhao, Z. Ling, H. Wang, S. Yu, and J. Zhang, "Evaluation of the best single-energy scanning in energy spectrum CT in lower extremity arteriography," *Experimental and Therapeutic Medicine*, Jun. 2019, doi: 10.3892/etm.2019.7666.
- [19] C. H. McCollough, S. Leng, L. Yu, and J. G. Fletcher, "Dual- and Multi-Energy CT: Principles, Technical Approaches, and Clinical Applications," *Radiology*, vol. 276, no. 3, pp. 637–653, Sep. 2015, doi: 10.1148/radiol.2015142631.
- [20] J.-H. Lee, D.-H. Kim, S.-N. Jeong, and S.-H. Choi, "Detection and diagnosis of dental caries using a deep learning-based convolutional neural network algorithm," *Journal of Dentistry*, vol. 77, pp. 106–111, Oct. 2018, doi: 10.1016/j.jdent.2018.07.015.
- [21] J. Jayapradha, S. Sourav, D. Singh, and M. U. Devi, "Detection of brain tumours using deep learning model," *AIP conference proceedings*, vol. 3075, pp. 020209–020209, Jan. 2024, doi: <https://doi.org/10.1063/5.0217153>.
- [22] M. Sia, K.-W. Ng, S.-C. Haw, and J. Jayaram, "Chronic disease prediction chatbot using deep learning and machine learning algorithms," *Bulletin of Electrical Engineering and Informatics*, vol. 14, no. 1, pp. 742–751, Nov. 2024, doi: 10.11591/eei.v14i1.8462.
- [23] X. Lu, Y. A. Nanehkaran, and M. Karimi Fard, "A Method for Optimal Detection of Lung Cancer Based on Deep Learning Optimized by Marine Predators Algorithm," *Computational Intelligence and Neuroscience*, vol. 2021, no. 1, Jan. 2021, doi: 10.1155/2021/3694723.

BIOGRAPHIES OF AUTHORS

	<p>Jayapradha J is an Assistant Professor at the department of Computing Technologies, SRMIST. She had completed her Ph.D(CSE) in Privacy Preservation. and has published many research articles on ML, data mining, and privacy. She has 6 patents published and 2 patents granted in the field of ML and data privacy. Her research interests include ML, databases, and privacy. She can be contacted at email: jayapraj@srmist.edu.in</p>
	<p>Su-Cheng Haw is Professor at Faculty of Computing and Informatics, Multimedia University, where she leads several funded projects on the XML databases. Her research interests include XML databases, query optimization, data modeling, semantic web, and recommender system. She can be contacted at email: sucheng@mmu.edu.my</p>
	<p>Palanichamy Naveen joined the Faculty of Computing and Informatics, Multimedia University after receiving Ph.D from Curtin University, Malaysia. She received her Bachelor of Engineering (CSE) and Master of Engineering (CSE) from Anna University, India. Her research interests include Smart Grid, Cloud Computing, ML, DL and Recommender system. She can be contacted at email: p.naveen@mmu.edu.my</p>

	<p>Senthil Kumar Thillaigovindhan graduated with a bachelor's degree in Electronics and Communication Engineering and a master's degree in computer science and engineering in 2004 and 2006, respectively. He completed his Ph.D. in CSE from SRMIST, Chennai, 2019. His areas of expertise include wireless communication, network security, ML, the Internet of Things, and vehicular networks. He can be contacted at email: senthilt2@srmist.edu.in</p>
	<p>Mutaz Al-Tarawneh is an associate professor of computer engineering at Mutah University. He has obtained his MSc and PhD degrees in Computer Engineering from Southern Illinois University, USA in 2008 and 2010, respectively. His current research interests include computer architecture, real-time systems and cloud computing. He can be reached at email: mutaz.altarawneh@mutah.edu.jo</p>